ADVANCED ENERGY MATERIALS

Supporting Information

for *Adv. Energy Mater.,* DOI: 10.1002/aenm.201701272

Annulated Dialkoxybenzenes as Catholyte Materials for Non-aqueous Redox Flow Batteries: Achieving High Chemical Stability through Bicyclic Substitution

Jingjing Zhang, Zheng Yang, Ilya A. Shkrob, Rajeev S. Assary, Siu on Tung, Benjamin Silcox, Wentao Duan, Junjie Zhang, Chi Cheung Su, Bin Hu, Baofei Pan, Chen Liao, Zhengcheng Zhang, Wei Wang, Larry A. Curtiss, Levi T. Thompson, Xiaoliang Wei, and Lu Zhang**

Supporting Information

Annulated Dialkoxybenzenes as Catholyte Materials for Nonaqueous Redox Flow Batteries: Achieving High Chemical Stability through Bicyclic Substitution

Jingjing Zhang, Zheng Yang, Ilya A. Shkrob, Rajeev S. Assary, Siu on Tung, Benjamin Silcox, Wentao Duan, Junjie Zhang, Chi Cheung Su, Bin Hu, Baofei Pan, Chen Liao, Zhengcheng Zhang, Wei Wang, Larry A. Curtiss, Levi T. Thompson, Xiaoliang Wei, and Lu Zhang**

Chemical Sciences and Engineering Division, Argonne National Laboratory, 9700 South Cass Avenue, Argonne, IL 60439, USA
Energy & Environmental Directorate, Pacific Northwest National Laboratory, Richland, WA 99352, USA
Email: xiaoliang.wei@pnnl.gov
Materials Science Division, Argonne National Laboratory, 9700 South Cass Avenue, Argonne, IL 60439, USA
Department of Chemical Engineering, University of Michigan, 2300 Hayward St, Ann Arbor, MI 48109, USA

1. Synthesis and Characterization

General Considerations

The following chemicals were purchased from commercial sources and used as received: dicyclopentadiene (Sigma-Aldrich), 1,4-benzoquinone (Sigma-Aldrich), 1,3-cyclohexadiene (Sigma-Aldrich), palladium on carbon (Sigma-Aldrich), sodium hydride (Sigma-Aldrich) and 2-bromoethyl methyl ether (Sigma-Aldrich). 1,4,4a,5,8,8a,9a,10a-octahydro-1,4:5,8-dimethanoanthracene-9,10-dione, dodecahydro-1,4:5,8-dimethano-anthracene-9,10-dione, 1,2,3,4,5,6,7,8-octahydro-1,4:5,8-dimethanoanthracene-9,10-diol, 1,4,4a,5,8,8a,9a,10a-octahydro-1,4:5,8-diethano-anthracene-9,10-dione, dodecahydro-1,4:5,8-diethanoanthracene-9,10-dione, 1,2,3,4,5,6,7,8-octahydro-1,4:5,8-diethanoanthra-cene-9,10-diol and 2-methoxyethyl tosylate were prepared using previously reported procedures.[1, 2]

All synthetic manipulations were performed in standard air-free conditions under an atmosphere of dry nitrogen gas with magnetic stirring unless otherwise mentioned. Flash chromatography was performed using silica gel (230-400 mesh) as the stationary phase. NMR spectra were acquired on a Bruker Avance DPX-300 spectrometer (300 Hz for ^{1}H). Chemical shifts are reported relative to the tetramethylsilane.

9,10-bis(2-methoxyethoxy)-1,2,3,4,5,6,7,8-octahydro-1,4:5,8-dimethanenoanthracene (BODMA)

To an ice-cold solution of *p*-benzoquinone (7.0 g, 65 mmol) in 70 mL of ethanol was added freshly prepared cyclopentadiene (8.6 g, 130 mmol), and the mixture was stirred for 30 min.

The white solid was filtered and washed with cold ethanol (20 mL) to yield 1,4,4a,5,8,8a,9a,10a-octahydro-1,4:5,8-dimethanoanthracene-9,10-dione (15.0 g, 96.4%).

Then a solution of 1,4,4a,5,8,8a,9a,10a-octahydro-1,4:5,8-dimethanoanthracene-9,10-dione (6.0 g, 25 mmol) in 80 mL of mixture of ethanol and ethyl acetate (1:1 v/v) containing 10 wt% Pd/C catalyst was hydrogenated at room temperature. The reaction was monitored using gas chromatography - mass spectrometry. Upon the full consumption of the starting material, the catalyst was separated by filtration through a short pad of Celite followed by rinsing with dichloromethane. The filtrate was concentrated *in vacuo* to give dodecahydro-1,4:5,8-dimethanoanthracene-9,10-dione (6.0 g, 99%).

Dodecahydro-1,4:5,8-dimethanoanthracene-9,10-dione (3.6 g, 14.6 mmol) was dissolved in 20 mL of dry chloroform at room temperature and a solution of Br_2 (2.3g, 14.6 mmol) in 20 mL of chloroform was added dropwise over 30 min. White precipitate was observed upon addition of Br_2. The resulting suspension was stirred at room temperature for additional 2 h. Most of HBr produced in the reaction was removed by bubbling N_2 through the reaction mixture. The resulting suspension was cooled in a dry ice - acetone bath, and the precipitate was filtered *in vacuo* to give 1,2,3,4,5,6,7,8-octahydro-1,4:5,8-dimethanoanthracene-9,10-diol (3.1 g, 89%).

In the last step, 1,2,3,4,5,6,7,8-octahydro-1,4:5,8-dimethanoanthracene-9,10-diol (1.5 g, 6.19 mmol) was dissolved in ethanol (30 mL). Potassium hydroxide (1.39 g, 24.8 mmol) in 12 mL water and 2-methoxyethyl tosylate (2.9 g, 12.4 mmol) were added to the reaction mixture. The reaction mixture was refluxed overnight. Then reaction mixture was cooled to room temperature and extracted with dichloromethane. The organic layer was then dried over Na_2SO_4. The crude product was recrystallized from hexane and dichloromethane to give 9,10-bis(2-methoxyethoxy)-1,2,3,4,5,6,7,8-octahydro-1,4:5,8-dimethanenoanthracene (2.0 g, 88%).

9,10-bis(2-methoxyethoxy)-1,2,3,4,5,6,7,8-octahydro-1,4:5,8-diethanoanthracene (BODEA)

To a solution of *p*-benzoquinone (10.0 g, 92 mmol) in 100 mL of ethanol was added 1,3-cyclohexyaldiene (14.8 g, 185 mmol) at room temperature. The reaction mixture was refluxed overnight. The white solid was collected by filtration and rinsed with cold ethanol (25 mL) to yield 1,4,4a,5,8,8a,9a,10a-octahydro-1,4:5,8-diethano-anthracene-9,10-dione (20.1 g, 81%).

Then a solution of 1,4,4a,5,8,8a,9a,10a-octahydro-1,4:5,8-diethano-anthracene-9,10-dione (20.1 g, 75 mmol) in 200 mL of mixture of ethanol and ethyl acetate (1:1, v/v) containing 10 wt% Pd/C was hydrogenated at room temperature. The reaction was monitored by GC-MS. Upon the full consumption of the starting material, the catalyst was separated by filtration through a short pad of Celite followed by rinsing with dichloromethane. The filtrate was concentrated *in vacuo* to give dodecahydro-1,4:5,8-diethanoanthracene-9,10-dione (21.5 g, 95%).

Dodecahydro-1,4:5,8-diethanoanthracene-9,10-dione (3.6 g, 14.6 mmol) was dissolved in 20 mL of dry chloroform at room temperature and a solution of Br_2 (2.3 g, 14.6 mmol) in 20 mL of chloroform was added dropwise over 30 min. White precipitate was observed upon addition of Br_2. The resulting suspension was stirred at room temperature for two more hours. Most of HBr produced in the reaction was blown off by bubbling N_2 through the reaction mixture. The resulting suspension was cooled in a dry ice - acetone bath, and the precipitate

was filtered *in vacuo* to give 1,2,3,4,5,6,7,8-octahydro-1,4:5,8-diethanoanthracene-9,10-diol (3.5 g, 99%).

In the last step, 1,2,3,4,5,6,7,8-octahydro-1,4:5,8-diethanoanthracene-9,10-diol (1.5 g, 5.6 mmol) was dissolved in ethanol (36 mL). Potassium hydroxide (1.3 g, 22.4 mmol) in 11 mL water and 2-methoxyethyl tosylate (2.6 g, 11.2 mmol) were added to the reaction mixture. The reaction mixture was refluxed overnight. Then reaction mixture was cooled to room temperature and extracted with dichloromethane. The organic layer was then dried over Na_2SO_4. The crude product was recrystallized from hexane and dichloromethane to give 9,10-bis(2-methoxyethoxy)-1,2,3,4,5,6,7,8-octahydro-1,4:5,8-diethanoanthracene (1.5 g, 72%).

Hexachloroantimonate 9,10-bis(2-methoxyethoxy)-1,2,3,4,5,6,7,8-octahydro-1,4:5,8-dimethanenoanthracene salt (BODMA$^{+\bullet}$ $SbCl_6^-$)

The hexachloroantimonate salt of **BODMA** was prepared according to a reported procedure.[1] $SbCl_5$ (0.3 g, 1.1 mmol) was slowly added in portions to a solution of **BODMA** (0.2 g, 0.5 mmol) in 4 mL dry dichloromethane at -78 ^oC. Bright orange precipitate was formed immediately, and the residue was collected *via* filtration. The orange crystals were rinsed with the minimum volume of diethyl ether three times and dried *in vacuo* with a nearly quantitative yield (0.4 g, 99%).

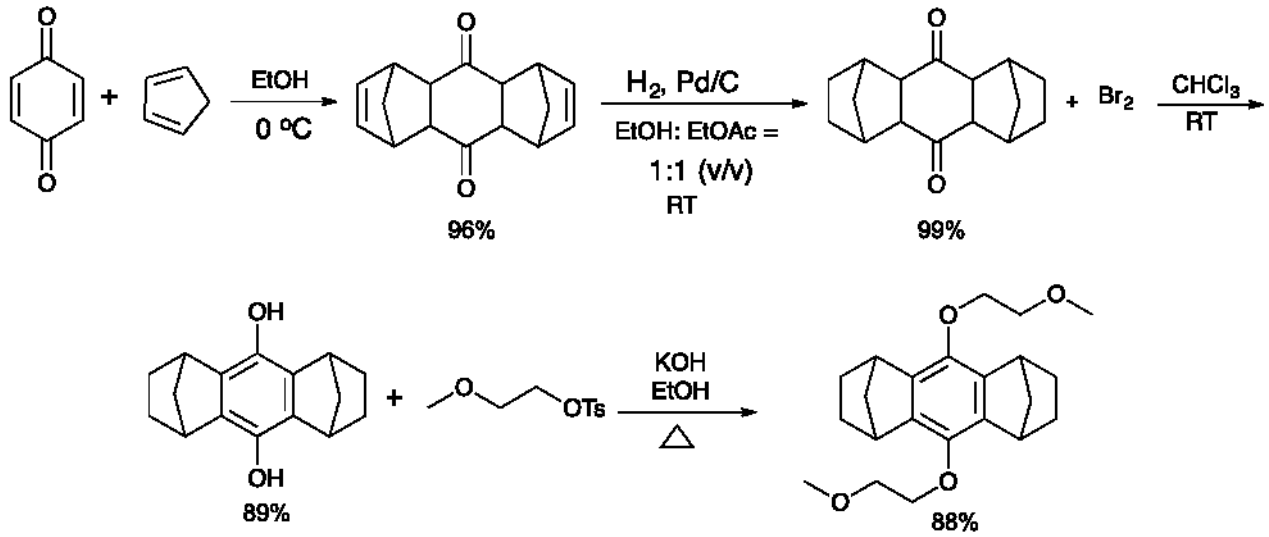

Scheme S1. The synthesis of **BODMA**.

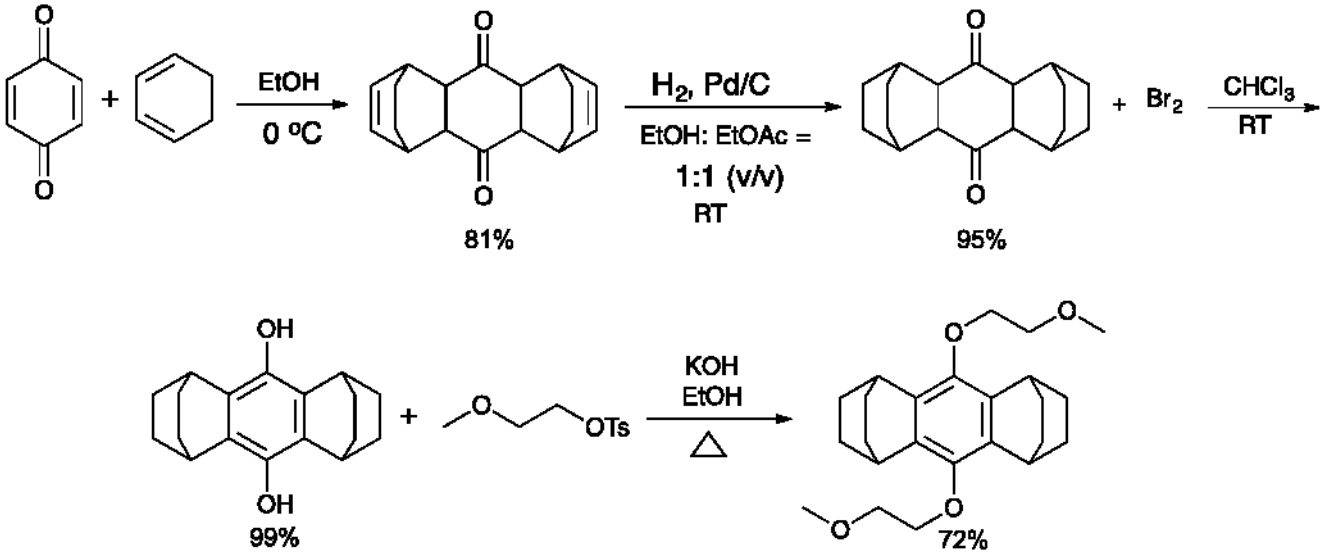

Scheme S2. The synthesis of **BODEA**.

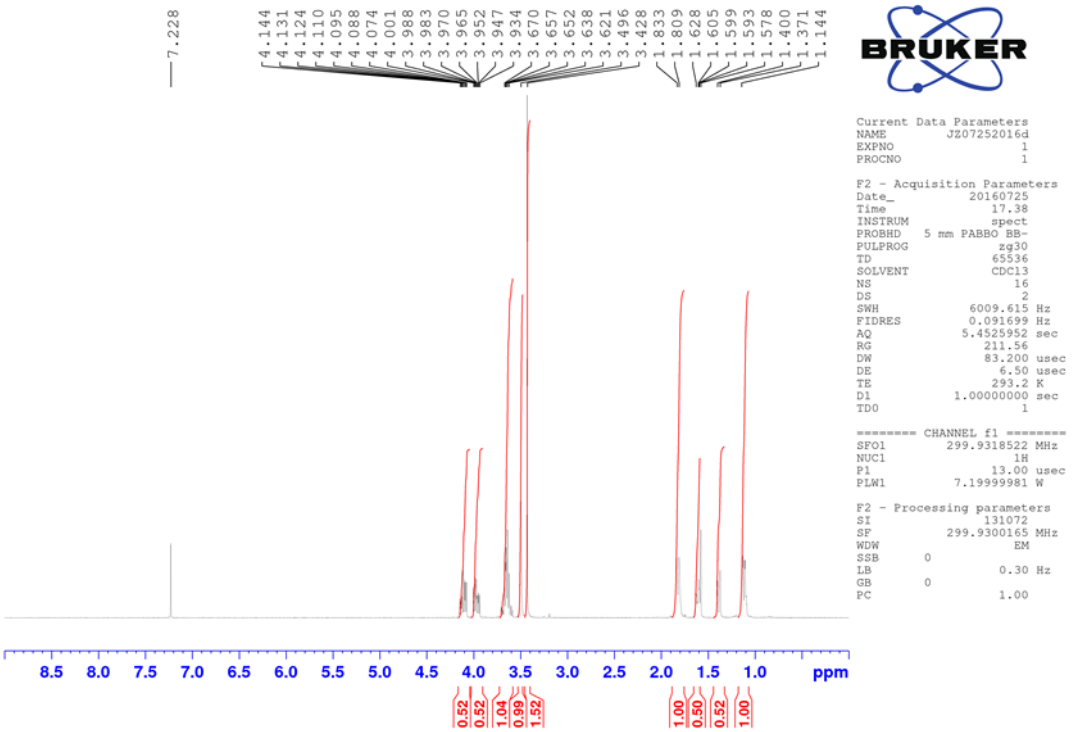

Figure S1. ^{1}H NMR spectrum of **BODMA** in $CDCl_3$.

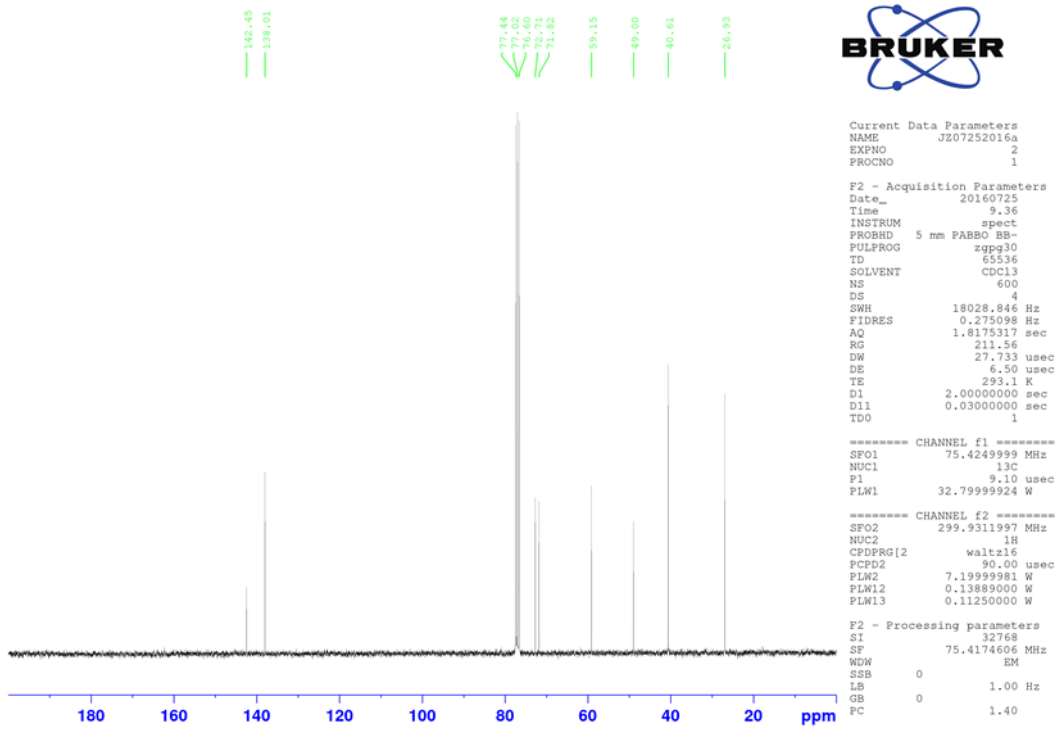

Fig S2. ^{13}C NMR spectrum of **BODMA** in $CDCl_3$.

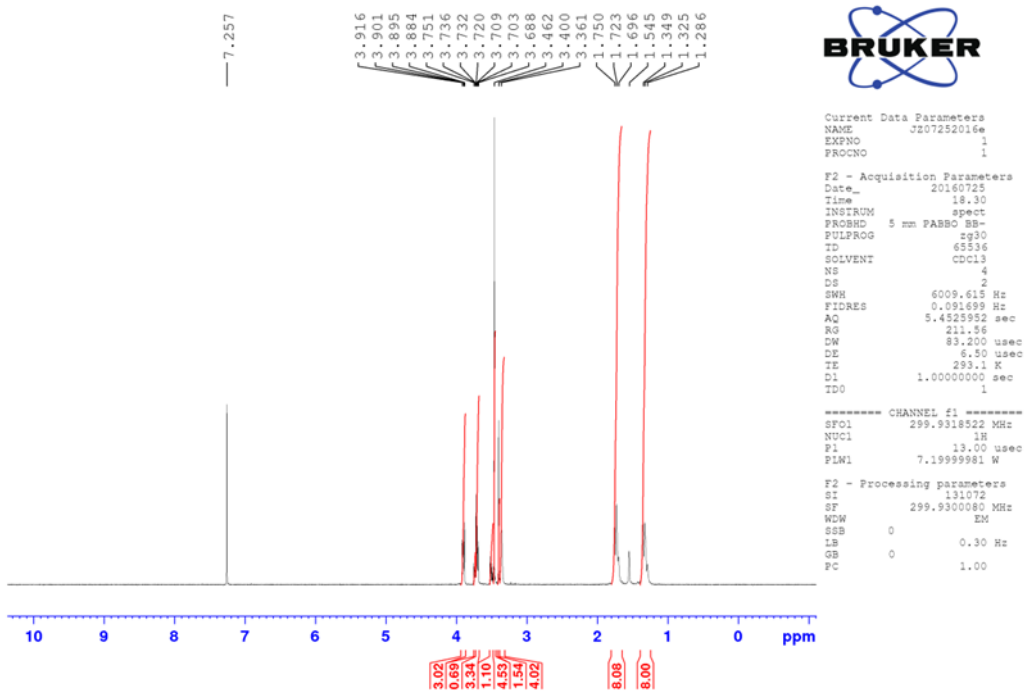

Figure S3. ^{1}H NMR spectrum of **BODEA** in $CDCl_3$.

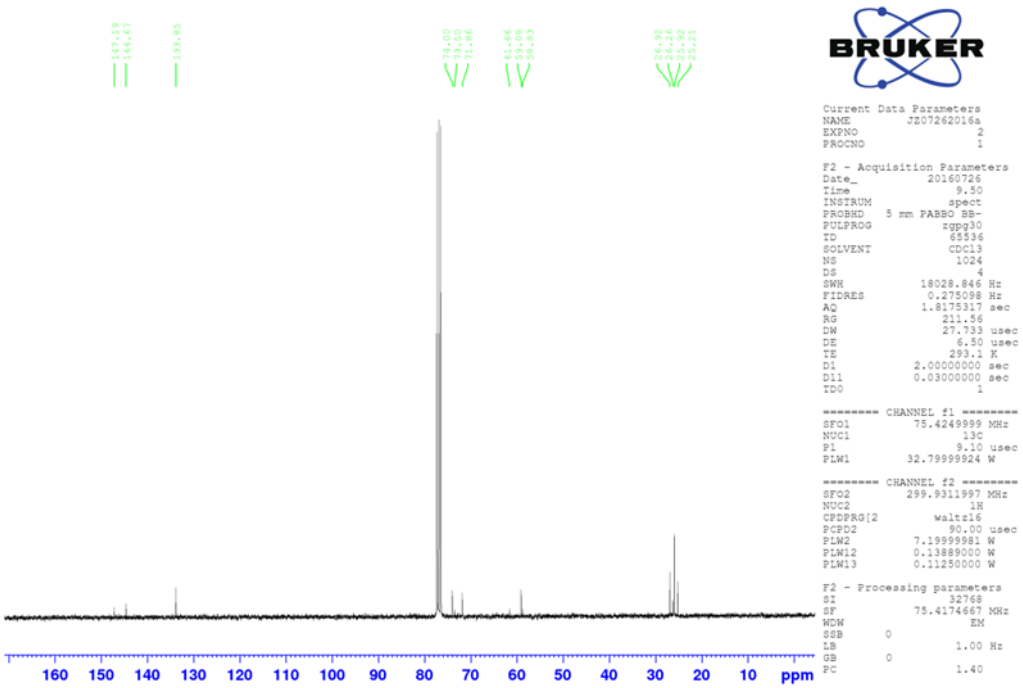

Figure S4. ^{13}C NMR spectrum of **BODEA** in $CDCl_3$.

2. Cyclic Voltammetry

Cyclic voltammetry was conducted in three-electrode cells. A Pt working electrode (2 mm diameter), a Li metal reference electrode, and a Li metal counter electrode were used in a cell containing the solutions of the catholyte molecules in Electrolyte A at 25 ^{o}C. All measurements were with iR compensation using CHI660D Potentiostat.

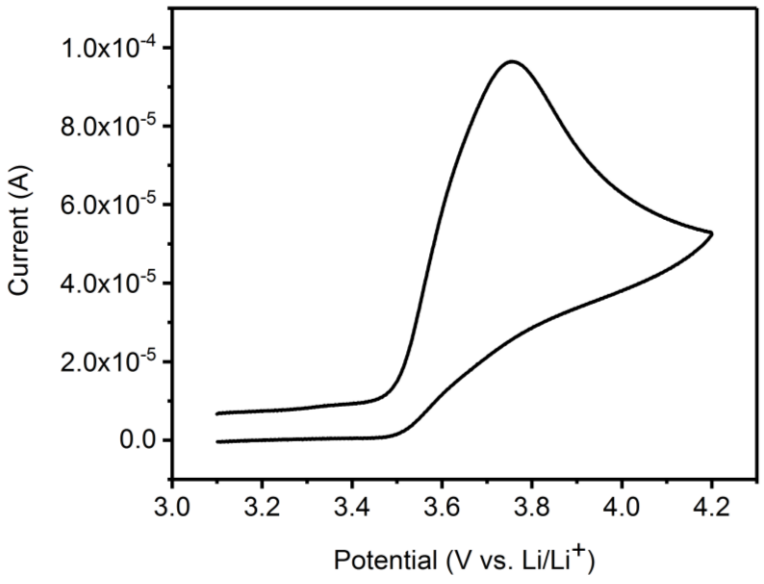

Figure S5. Cyclic voltammogram of 10 mM **DMTM** in Electrolyte A in a cell equipped with the Pt/Li/Li electrodes.

3. Diffusion coefficient measurements.

Diffusion coefficients were obtained from the cyclic voltammograms using the Randles-Sevcik equation:[3]

$i_{AP} = (268{,}600)n^{3/2}AD^{1/2}Cv^{1/2}$ (Equation S1)

where i_{AP} is the anodic peak current, n is the number of electrons, A is the electrode area, D is the diffusion coefficient of the analyte, C is the concentration of the analyte, and v is the potential sweep rate. In Fig S5, i_{AP} is plotted vs. $v^{1/2}$. The linearity suggests diffusion-controlled electrochemical redox reaction. The diffusion coefficients were estimated from the slopes of the least-squares lines shown in this plot using eq. S1 above.

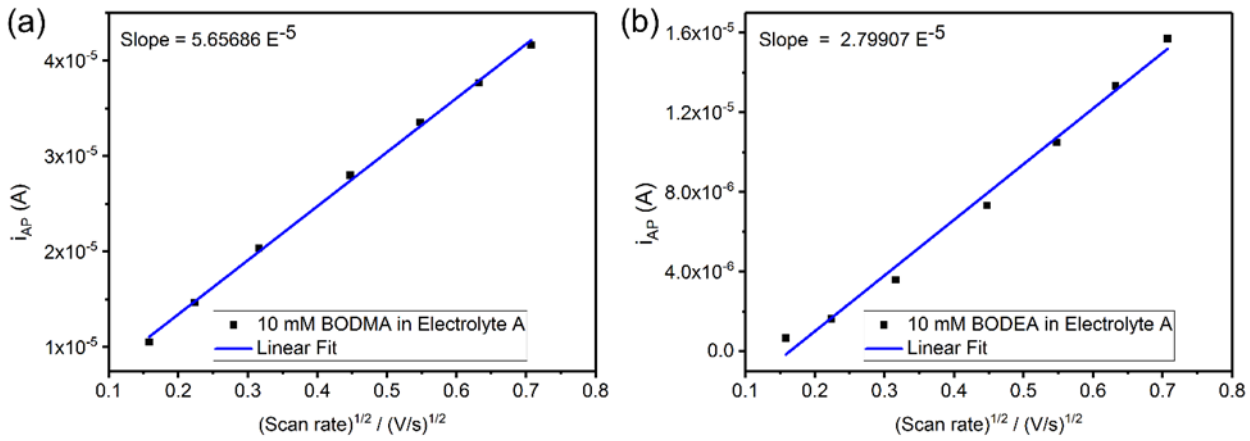

Figure S6. Plots of i_{AP} vs. $v^{1/2}$ for 10 mM (a) **BODMA** and (b) **BODEA** in Electrolyte A.

4. DFT

All computations were performed using the Gaussian 09 software. The B3LYP/6-31+G(d,p) level of density functional theory was used to compute the optimized structure, electronic energy, vibrational frequencies, and free energy corrections for all gas phase species.

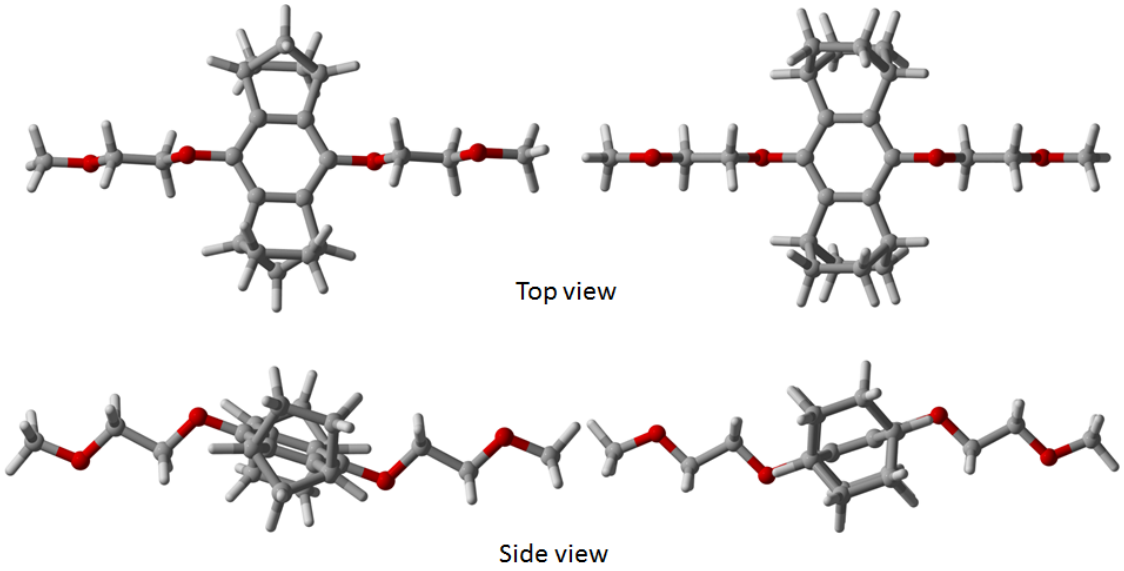

Fig S7. Optimized structures of the gas phase **BODMA** (*left*) and **BODEA** (*right*) from the density functional theory calculations.

5. EPR

BODMA and **BODEA** were electrochemically oxidized using 5 mM solutions in a carbonate electrolyte (3:7 w/w mixture of ethylene carbonate and ethyl methyl carbonate containing 1.2 M $LiPF_6$, defined as Gen 2 electrolyte). Alternatively, these molecules were chemically oxidized in dichloromethane using 1 mol.eq. phenyliodine bis(trifluoroacetate) (PIFA) or solid **BODMA**$^{+\bullet}$ $SbCl_6$ salt was introduced into the solutions. The time lag between the end of the electrolysis and sampling of the kinetic data was no more than 10 min. Continuous-wave EPR was used to observe radical cations *in situ* and study their decay kinetics. In these EPR experiments, 100 µL aliquots of oxidized liquid samples were placed in graduated glass capillaries and sealed inside glass tubes. The first-derivative EPR spectra were collected at 23 ^{o}C using a Bruker ESP300E X-band spectrometer operating at 9.45 GHz, the modulation frequency of 100 kHz, and the modulation amplitude of 0.2 G (1 G = 10^{-4} T). The analysis of the EPR spectra of the radical cations to estimate the proton hyperfine coupling constants (hfcc's) was carried out using WinSim program suite. EPR parameters obtained using electrochemical and chemical oxidation methods for the radical cations are summarized in Table S1. These parameters correspond to a radical cation with the central or axial symmetry, and the estimates for hfcc's are close to the ones predicted by our density functional theory calculations for these radical cations in the gas phase (section S4). For kinetic analyses, the EPR spectra were centered, background corrected, and then doubly integrated. The value of this integral *I(t)* was normalized by the value at *t=0*. The life time was defined as the delay time for the attainment of 50% decay. The time lag between the chemical preparations or the end of electrolytic oxidation and sampling of the kinetic data was 10-15 min or less. For most of the radical cations, this time lag can be neglected. For the short-lived species, the kinetics were exponential, so the location of the "zer time" is unimportant due to self-similarity of the exponential function.

Table S1.

EPR parameters determined for radical cations of BODMA and BODEA in liquid solutions, by chemical or electrochemical oxidation of the parent molecules.

Radical species	solution	(*g*-2) x10^{4} [c]	Isotropic hfcc, G (experiment) [d]
BODMA$^{+\bullet}$	PIFA, CH_2Cl_2	46	2H 3.911, 2H 3.502 2H 1.697, 2H 1.218
BODMA$^{+\bullet}$ $SbCl_6^-$ [a]	CH_2Cl_2	46	2H 3.755, 2H 3.482 2H 1.550, 2H 1.430
BODMA$^{+\bullet}$ $SbCl_6^-$ [a]	MeCN	52	2H 4.094, 2H 3.614 2H 1.604, 2H 1.247
BODMA$^{+\bullet}$ $SbCl_6^-$ [a,b]	carbonate	44	2H 4.092, 2H 3.624 2H 1.656, 2H 1.265
BODEA$^{+\bullet}$	PIFA, CH_2Cl_2	45	4H 2.494, 4H 0.727 4H 0.680
BODEA$^{+\bullet}$ [e]	carbonate	48	4H 2.629, 4H 0.719 4H 0.555

a) solution of the solid salts.
b) the same parameters were obtained by electrochemical oxidation of **BODMA** in a carbonate electrolyte;
c) *g*-factor for the radical cation;
d) hyperfine coupling constant, 1 G (Gauss) = 10^{-4} T;
e) electrochemical oxidation.

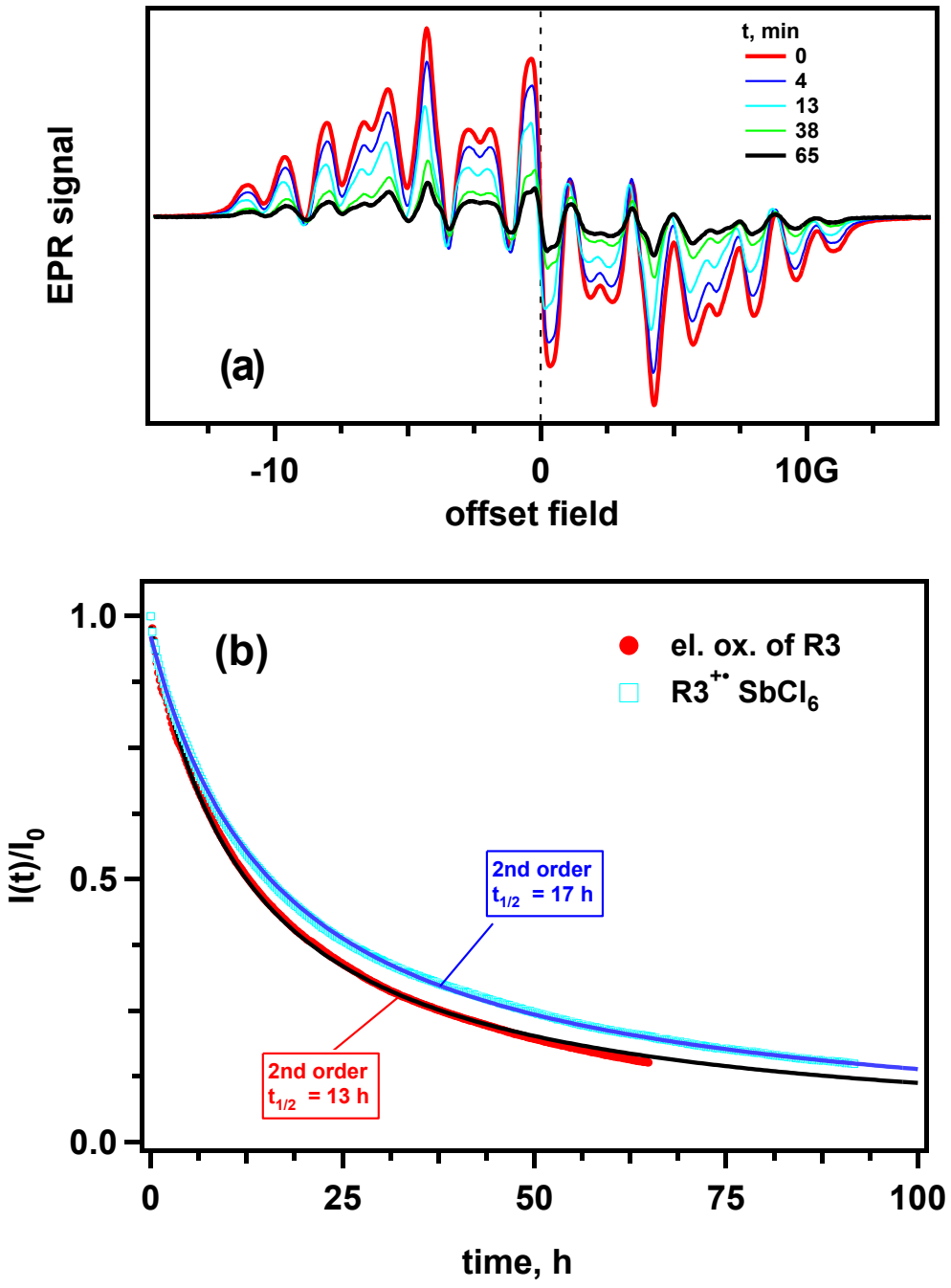

Figure S8. Time evolution of EPR signals and the normalized decay kinetics of **BODMA**$^{+\bullet}$ in Gen2 electrolyte. The radical cation was generated either by bulk electrolysis of 5 mM **BODMA** in a Li/C cell (with the state of charge nominally corresponding to 100% oxidation of the material) or by dissolving 5 mM **BODMA**$^{+\bullet}$ $SbCl_6^-$ in this electrolyte. In both cases, the decay kinetics corresponds to 2nd order decay of the radical cation, and the time constants of this decay are similar.

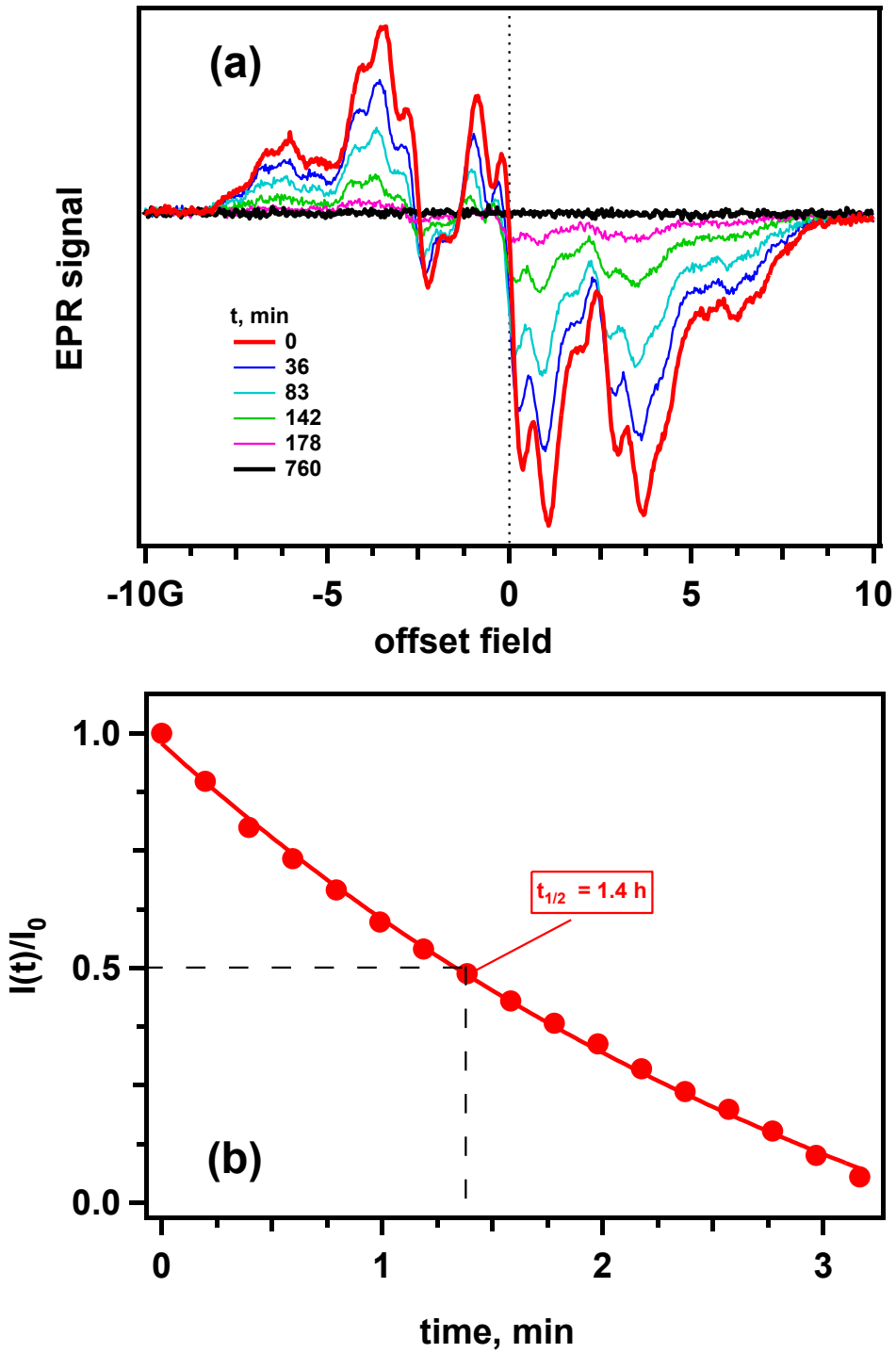

Figure S9. Time evolution of EPR signals (a) and the normalized decay kinetics (b) of **BODEA**$^{+\bullet}$ in Gen2 electrolyte. The radical cation was generated by electrolysis of 5 mM **BODEA** in a Li/C cell (with the state of charge nominally corresponding to 100% oxidation of the material).

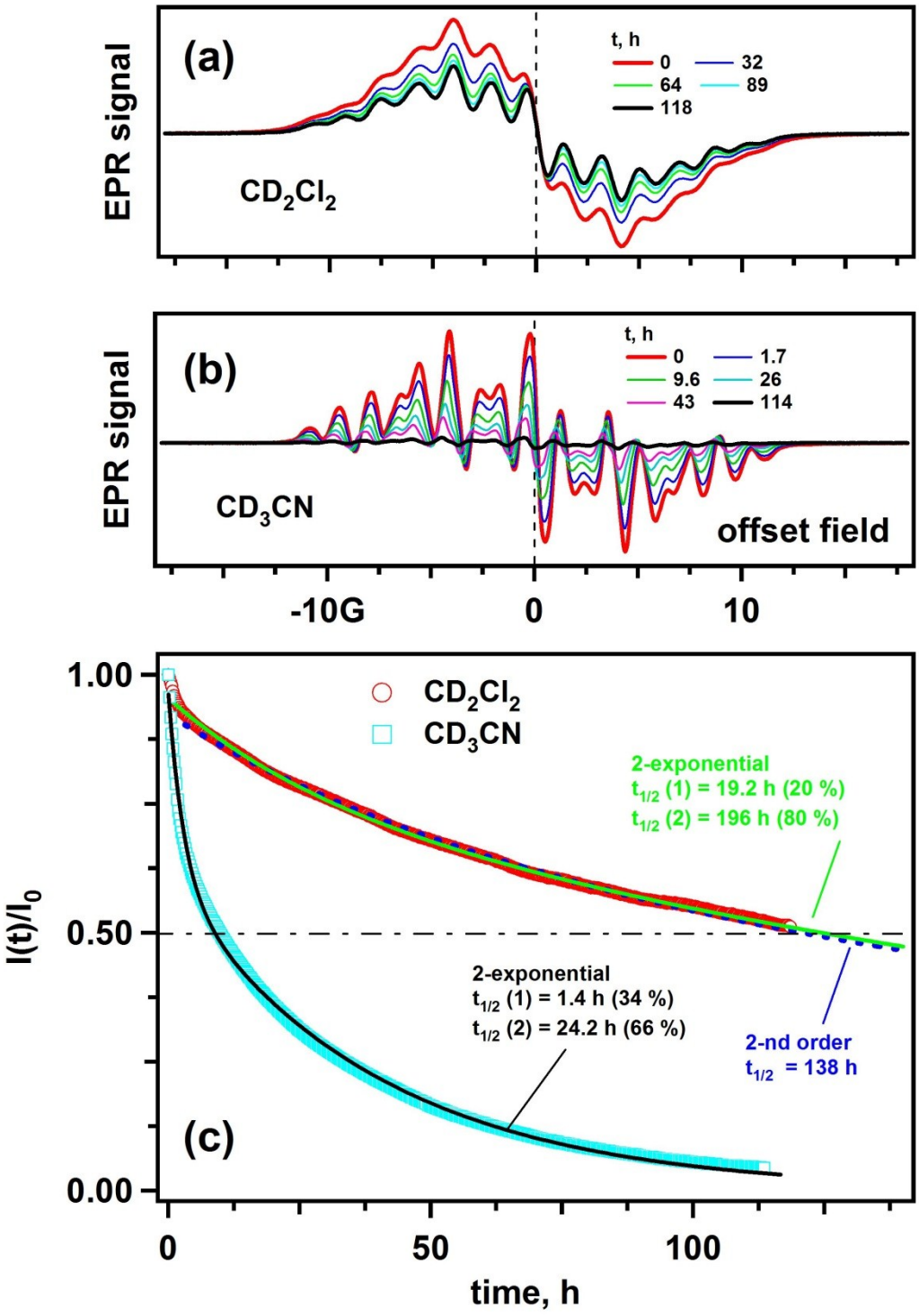

Figure S10. Time evolution of EPR signals from 5 mM **BODMA**$^{+\bullet}$ $SbCl_6^-$ in (a) dichloromethane-d_2 and (b) acetonitrile-d_3. The delay times are indicated in the plot. (c) Normalized decay kinetics of the doubly integrated EPR signals from the same solution (see the legend). The decay curves are fit by two-exponential dependences with the time constants given in the plot. For dichloromethane, second order decay kinetics also gives a good fit.

6. Hybrid flow cell cycling performance tests

The electrode compartments of the flow cells involved a hybrid anode, a graphite felt (GFD, 3 mm thick; SGL Group) at the cathode side, and a polyethylene-based microporous separator (800 µm thick, 57% porosity, 0.15 µm median pore size; Daramic) sandwiched in between (Fig S6a). The hybrid anode consisted of a graphite felt strip directly stacked on Li foil. Prior to use, the separator and the graphite felt were vacuum dried at 70 °C for 24 h to remove moisture. The active area of the flow cell was 20 cm^2. The electrolyte composition was 0.1 M **BODMA** in Electrolyte A containing 5 wt% fluoroethylene carbonate as additive to protect the anode. The hybrid anode was saturated with a static electrolyte that was not included in calculating the specific capacity or energy density. This static solution had the same composition as the catholyte solution. A flowing electrolyte (8 mL) was circulated through the graphite felt cathode by using a Masterflex L/S peristaltic pump (Cole-Parmer) at a flow rate of 50 mL/min. Charge/discharge cycling of the flow cell housed in an Ar-filled glove box at ~30°C was performed on a LAND battery tester (LanHe instruments, China). The calculation of specific capacity was based on the cycled capacity divided by the mass of redox materials in the catholyte solution.

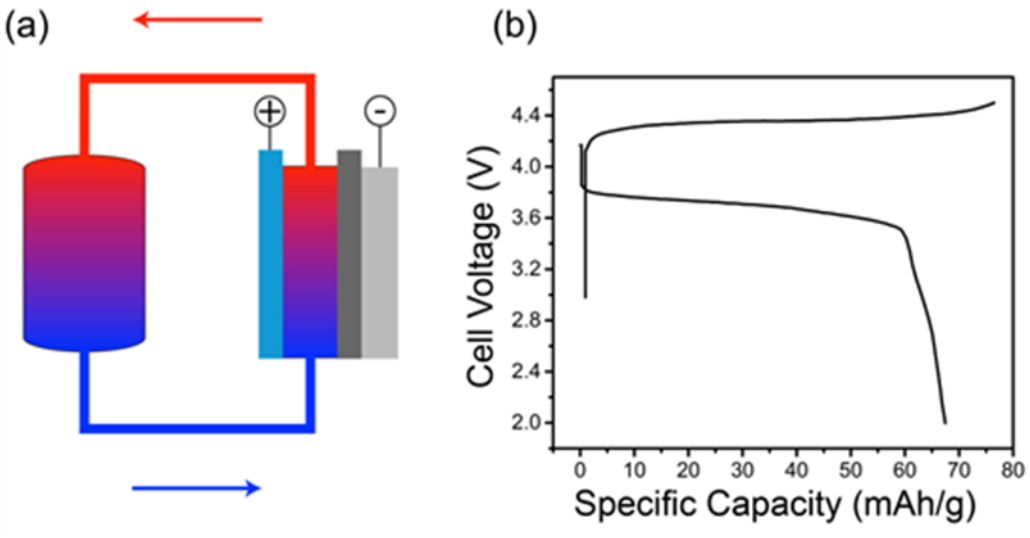

Figure S11. (a) Schematic drawing of the hybrid flow cell with a graphite felt cathode and a Li-graphite anode. (b) The representative charge/discharge voltage curve for the flow cell with 0.1 M **BODMA**.

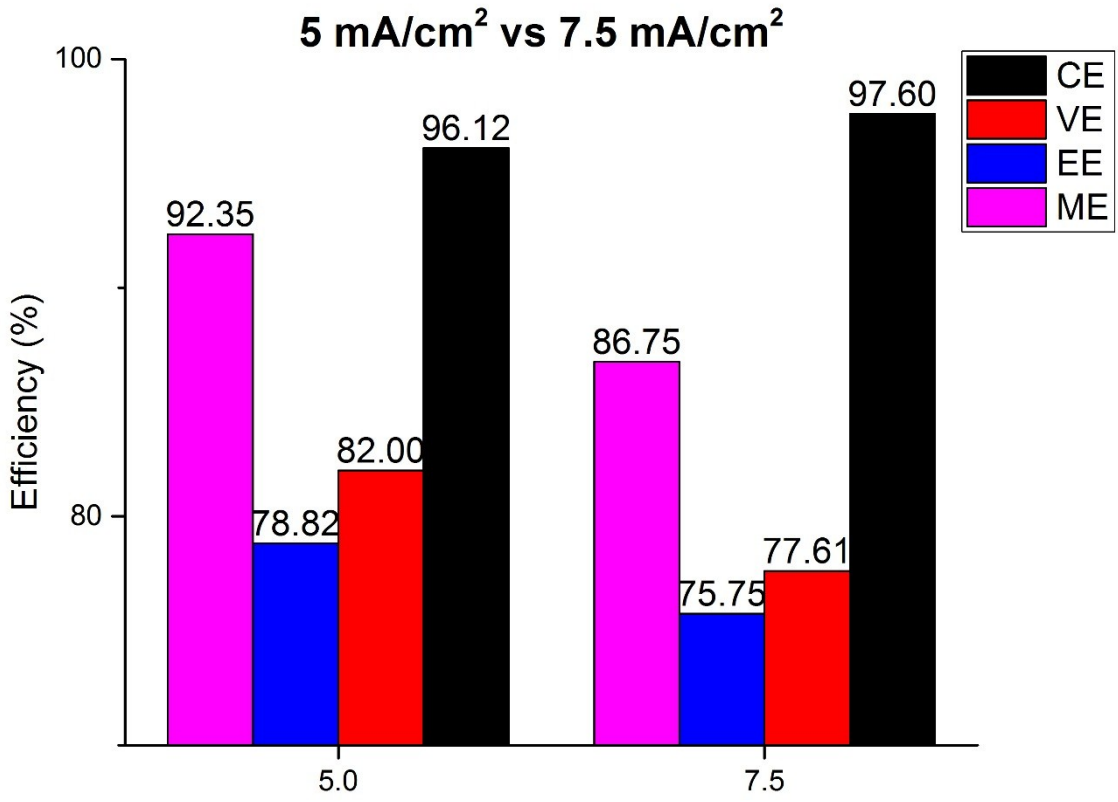

Figure S12. Comparison of the performance of the Li/BODMA hybrid flow cells operated at current densities of 5 mA/cm^2 (*to the left*) and 7.5 mA/cm^2 (*to the right*). ME is material utilization efficiency defined as the percentage of the discharge capacity to the theoretical capacity.

7. X-ray Crystallography

Single crystals of **BODMA** with dimensions of ~0.45×0.40×0.17 mm^3 and **BODEA** (~0.50×0.30×0.24 mm^3) were affixed to the tip of a glass fiber and mounted on a Bruker AXS SMART three-circle diffractometer equipped with an APEX II CCD detector and Mo *Kα* radiation (λ=0.71073 Å). Preliminary lattice parameters and orientation matrices were obtained from three sets of frames. Full data sets for structural analysis were collected at room temperature with a detector distance of 50 mm. Data integration and cell refinement were performed by the SAINT program of the APEX2 software and multi-scan absorption corrections were applied using the SCALE program for area detector.[4] The structures were solved by direct methods and refined by full matrix least-squares methods on F^2. All non-hydrogen atoms were refined with anisotropic thermal parameters, and the refinements converged for $I > 2\sigma(I)$. Calculations were performed using the SHELXTL crystallographic software package.[5] Details of crystal parameters, data collection and structure refinement at each temperature are summarized in Tables S2 and S7. Atomic positions at each temperature are listed in Tables S3 and S8. Additional information in the form of CIF has also been supplied in Tables S4 to S11.

Table S2. Crystal data and structure refinement for BODMA.

Empirical formula	C11 H15 O2
Formula weight	179.23
Temperature	295(2) K
Wavelength	0.71073 Å
Crystal system	Monoclinic
Space group	P 21/c
Unit cell dimensions	a = 9.3489(10) Å b = 9.9499(12) Å β= 109.998(5)°. c = 11.1736(12) Å
Volume	976.71(19) $Å^3$
Z	4
Density (calculated)	1.219 Mg/m^3
Absorption coefficient	0.082 mm^{-1}
F(000)	388
Crystal size	0.450 x 0.400 x 0.170 mm^3
Theta range for data collection	2.318 to 30.832°.
Index ranges	-13<=h<=13, -14<=k<=14, -16<=l<=16
Reflections collected	12849
Independent reflections	3064 [R(int) = 0.0261]
Completeness to theta = 25.242°	100.0 %
Refinement method	Full-matrix least-squares on F^2
Data / restraints / parameters	3064 / 0 / 127
Goodness-of-fit on F^2	1.062
Final R indices [I>2σ(I)]	R1 = 0.0471, wR2 = 0.1297
R indices (all data)	R1 = 0.0714, wR2 = 0.1452
Largest diff. peak and hole	0.246 and -0.160 $e.Å^{-3}$

Table S3. Atomic coordinates (x 10^4) and equivalent isotropic displacement parameters U(eq) ($Å^2$x 10^3) for BODMA.

	x	y	z	U(eq) [a]
O(001)	4584(1)	4721(1)	7360(1)	43(1)
O(002)	2456(1)	4033(1)	8624(1)	71(1)
C(003)	4786(1)	4830(1)	6190(1)	35(1)
C(004)	6413(1)	4802(1)	4898(1)	37(1)
C(005)	6204(1)	4633(1)	6071(1)	36(1)
C(006)	7726(1)	4187(1)	7010(1)	47(1)
C(007)	3864(2)	3409(1)	8846(1)	48(1)
C(008)	8067(1)	4465(2)	5117(1)	51(1)
C(009)	4210(2)	3396(1)	7636(1)	50(1)
C(00A)	8808(1)	4985(2)	6491(1)	57(1)
C(00B)	7996(2)	2738(2)	6638(1)	62(1)
C(00C)	8231(2)	2933(2)	5341(2)	66(1)
C(00D)	2011(2)	4071(2)	9694(2)	73(1)

a) one third of the trace of the U^{ij} tensor.

Table S4. Bond lengths [Å] and angles [°] for BODMA.

O(001)-C(003)	1.3878(12)
O(001)-C(009)	1.4247(14)
O(002)-C(00D)	1.3952(16)
O(002)-C(007)	1.3983(16)
C(003)-C(005)	1.3910(14)
C(003)-C(004)#1	1.3911(16)
C(004)-C(003)#1	1.3911(16)
C(004)-C(005)	1.3996(15)
C(004)-C(008)	1.5183(15)
C(005)-C(006)	1.5167(15)
C(006)-C(00B)	1.546(2)
C(006)-C(00A)	1.5462(19)
C(006)-H(006)	0.9800
C(007)-C(009)	1.4937(17)
C(007)-H(00A)	0.978(17)
C(007)-H(00B)	0.985(17)
C(008)-C(00A)	1.5421(19)
C(008)-C(00C)	1.544(2)
C(008)-H(008)	0.9800
C(009)-H(00C)	0.9700
C(009)-H(00D)	0.9700
C(00A)-H(00E)	0.9700
C(00A)-H(00F)	0.9700
C(00B)-C(00C)	1.550(2)
C(00B)-H(00G)	0.9700
C(00B)-H(00H)	0.9700

C(00C)-H(00I)	0.9700
C(00C)-H(00J)	0.9700
C(00D)-H(00K)	0.9600
C(00D)-H(00L)	0.9600
C(00D)-H(00M)	0.9600

C(003)-O(001)-C(009)	113.52(8)
C(00D)-O(002)-C(007)	113.50(11)
O(001)-C(003)-C(005)	121.36(10)
O(001)-C(003)-C(004)#1	120.99(9)
C(005)-C(003)-C(004)#1	117.60(10)
C(003)#1-C(004)-C(005)	121.37(9)
C(003)#1-C(004)-C(008)	132.14(10)
C(005)-C(004)-C(008)	106.45(10)
C(003)-C(005)-C(004)	121.03(10)
C(003)-C(005)-C(006)	132.38(10)
C(004)-C(005)-C(006)	106.55(9)
C(005)-C(006)-C(00B)	106.70(10)
C(005)-C(006)-C(00A)	99.78(10)
C(00B)-C(006)-C(00A)	100.93(11)
C(005)-C(006)-H(006)	115.8
C(00B)-C(006)-H(006)	115.8
C(00A)-C(006)-H(006)	115.8
O(002)-C(007)-C(009)	108.99(11)
O(002)-C(007)-H(00A)	110.9(10)
C(009)-C(007)-H(00A)	108.1(10)
O(002)-C(007)-H(00B)	109.2(9)
C(009)-C(007)-H(00B)	109.9(9)
H(00A)-C(007)-H(00B)	109.8(13)
C(004)-C(008)-C(00A)	99.91(9)
C(004)-C(008)-C(00C)	106.47(11)
C(00A)-C(008)-C(00C)	100.60(11)
C(004)-C(008)-H(008)	115.9
C(00A)-C(008)-H(008)	115.9
C(00C)-C(008)-H(008)	115.9
O(001)-C(009)-C(007)	109.46(10)
O(001)-C(009)-H(00C)	109.8
C(007)-C(009)-H(00C)	109.8
O(001)-C(009)-H(00D)	109.8
C(007)-C(009)-H(00D)	109.8
H(00C)-C(009)-H(00D)	108.2
C(008)-C(00A)-C(006)	94.16(10)
C(008)-C(00A)-H(00E)	112.9
C(006)-C(00A)-H(00E)	112.9
C(008)-C(00A)-H(00F)	112.9
C(006)-C(00A)-H(00F)	112.9
H(00E)-C(00A)-H(00F)	110.3
C(006)-C(00B)-C(00C)	102.88(11)
C(006)-C(00B)-H(00G)	111.2
C(00C)-C(00B)-H(00G)	111.2
C(006)-C(00B)-H(00H)	111.2

C(00C)-C(00B)-H(00H)	111.2
H(00G)-C(00B)-H(00H)	109.1
C(008)-C(00C)-C(00B)	103.75(11)
C(008)-C(00C)-H(00I)	111.0
C(00B)-C(00C)-H(00I)	111.0
C(008)-C(00C)-H(00J)	111.0
C(00B)-C(00C)-H(00J)	111.0
H(00I)-C(00C)-H(00J)	109.0
O(002)-C(00D)-H(00K)	109.5
O(002)-C(00D)-H(00L)	109.5
H(00K)-C(00D)-H(00L)	109.5
O(002)-C(00D)-H(00M)	109.5
H(00K)-C(00D)-H(00M)	109.5
H(00L)-C(00D)-H(00M)	109.5

Symmetry transformations used to generate equivalent atoms:
#1 -x+1,-y+1,-z+1

Table S5. Anisotropic displacement parameters U^{ij} ($Å^2 x\ 10^3$) for BODMA. The anisotropic displacement factor exponent takes the form: $-2\pi^2[\ h^2a^2U^{11} + ... + 2\ h\ k\ a\ b\ U^{12} + \ldots]$

	U^{11}	U^{22}	U^{33}	U^{23}	U^{13}	U^{12}
O(001)	56(1)	43(1)	38(1)	-1(1)	25(1)	-5(1)
O(002)	60(1)	105(1)	57(1)	25(1)	33(1)	25(1)
C(003)	39(1)	36(1)	34(1)	-1(1)	18(1)	-1(1)
C(004)	33(1)	41(1)	40(1)	0(1)	16(1)	2(1)
C(005)	34(1)	39(1)	37(1)	1(1)	13(1)	2(1)
C(006)	39(1)	59(1)	41(1)	4(1)	10(1)	7(1)
C(007)	56(1)	46(1)	47(1)	10(1)	25(1)	4(1)
C(008)	35(1)	70(1)	54(1)	5(1)	22(1)	8(1)
C(009)	67(1)	41(1)	52(1)	3(1)	32(1)	-1(1)
C(00A)	31(1)	78(1)	58(1)	2(1)	10(1)	-1(1)
C(00B)	58(1)	61(1)	66(1)	12(1)	19(1)	24(1)
C(00C)	58(1)	72(1)	72(1)	-2(1)	26(1)	28(1)
C(00D)	75(1)	92(1)	68(1)	6(1)	46(1)	8(1)

Table S6. Hydrogen coordinates (x 10^4) and isotropic displacement parameters U(eq) (Å^{2}x 10^3) for BODMA.

	x	y	z	U(eq)
H(006)	7868	4330	7911	57
H(008)	8485	4826	4489	62
H(00C)	5057	2796	7721	61
H(00D)	3332	3072	6944	61
H(00E)	8713	5950	6560	69
H(00F)	9864	4714	6874	69
H(00G)	7123	2170	6550	74
H(00H)	8891	2346	7263	74
H(00I)	9231	2627	5382	80
H(00J)	7465	2449	4669	80
H(00K)	1113	4614	9516	109
H(00L)	2815	4449	10399	109
H(00M)	1797	3175	9905	109
H(00A)	4677(19)	3900(17)	9485(16)	71(5)
H(00B)	3816(17)	2481(18)	9138(14)	67(4)

Table S7. Crystal data and structure refinement for BODEA.

Empirical formula	C12 H17 O2
Formula weight	193.25
Temperature	295(2) K
Wavelength	0.71073 Å
Crystal system	Monoclinic
Space group	P 21/c
Unit cell dimensions	a = 9.8958(4) Å b = 10.0991(4) Å β= 111.045(2)°. c = 11.2973(5) Å
Volume	1053.73(8) $Å^3$
Z	4
Density (calculated)	1.218 Mg/m^3
Absorption coefficient	0.081 mm^{-1}
F(000)	420
Crystal size	0.5 x 0.3 x 0.24 mm^3
Theta range for data collection	2.205 to 30.794°.
Index ranges	-14<=h<=13, -14<=k<=14, -16<=l<=16
Reflections collected	13960
Independent reflections	3298 [R(int) = 0.0253]
Completeness to theta = 25.242°	100.0 %
Refinement method	Full-matrix least-squares on F^2
Data / restraints / parameters	3298 / 0 / 136
Goodness-of-fit on F^2	1.033
Final R indices [I>2sigma(I)]	R1 = 0.0470, wR2 = 0.1275
R indices (all data)	R1 = 0.0712, wR2 = 0.1445
Largest diff. peak and hole	0.266 and -0.186 $e.Å^{-3}$

Table S8. Atomic coordinates (x 10^4) and equivalent isotropic displacement parameters U(eq) ($Å^2$x 10^3) for BODEA.

	x	y	z	U(eq)
O(001)	5456(1)	4745(1)	2709(1)	45(1)
O(002)	7316(1)	4192(1)	1275(1)	62(1)
C(003)	5238(1)	4848(1)	3861(1)	37(1)
C(004)	3659(1)	4680(1)	5066(1)	38(1)
C(005)	3901(1)	4527(1)	3926(1)	38(1)
C(006)	2583(1)	4036(1)	2856(1)	50(1)
C(007)	2153(1)	4280(1)	4970(1)	50(1)
C(008)	5952(2)	3465(1)	2507(1)	53(1)
C(009)	6112(2)	3423(1)	1241(1)	52(1)
C(00A)	1058(1)	5142(2)	3935(1)	63(1)
C(00B)	1358(2)	5038(2)	2695(1)	64(1)
C(00C)	7574(2)	4139(2)	138(1)	62(1)
C(00D)	1924(2)	2835(2)	4521(2)	64(1)
C(00E)	2131(2)	2694(2)	3238(1)	66(1)

Table S9. Bond lengths [Å] and angles [°] for BODEA.

O(001)-C(003)	1.3968(12)
O(001)-C(008)	1.4296(14)
O(002)-C(00C)	1.3981(15)
O(002)-C(009)	1.4105(17)
C(003)-C(005)	1.3899(15)
C(003)-C(004)#1	1.3929(15)
C(004)-C(003)#1	1.3929(15)
C(004)-C(005)	1.4003(14)
C(004)-C(007)	1.5092(15)
C(005)-C(006)	1.5084(15)
C(006)-C(00E)	1.537(2)
C(006)-C(00B)	1.539(2)
C(006)-H(006)	0.9800
C(007)-C(00D)	1.536(2)
C(007)-C(00A)	1.5453(18)
C(007)-H(007)	0.9800
C(008)-C(009)	1.4957(17)
C(008)-H(00A)	0.9700
C(008)-H(00B)	0.9700
C(009)-H(00C)	0.940(16)
C(009)-H(00D)	1.016(16)
C(00A)-C(00B)	1.537(2)
C(00A)-H(00E)	0.9700
C(00A)-H(00F)	0.9700
C(00B)-H(00G)	0.9700
C(00B)-H(00H)	0.9700
C(00C)-H(00I)	0.9600
C(00C)-H(00J)	0.9600
C(00C)-H(00K)	0.9600
C(00D)-C(00E)	1.541(2)
C(00D)-H(00L)	0.9700
C(00D)-H(00M)	0.9700
C(00E)-H(00N)	0.9700
C(00E)-H(00O)	0.9700

C(003)-O(001)-C(008)	113.17(8)
C(00C)-O(002)-C(009)	112.61(10)
C(005)-C(003)-C(004)#1	119.83(9)
C(005)-C(003)-O(001)	120.05(9)
C(004)#1-C(003)-O(001)	120.08(9)
C(003)#1-C(004)-C(005)	119.94(9)
C(003)#1-C(004)-C(007)	126.80(10)
C(005)-C(004)-C(007)	113.25(10)
C(003)-C(005)-C(004)	120.22(9)
C(003)-C(005)-C(006)	126.85(10)
C(004)-C(005)-C(006)	112.90(10)
C(005)-C(006)-C(00E)	108.61(10)
C(005)-C(006)-C(00B)	107.24(10)

C(00E)-C(006)-C(00B)	108.49(12)
C(005)-C(006)-H(006)	110.8
C(00E)-C(006)-H(006)	110.8
C(00B)-C(006)-H(006)	110.8
C(004)-C(007)-C(00D)	107.61(11)
C(004)-C(007)-C(00A)	108.09(10)
C(00D)-C(007)-C(00A)	107.76(12)
C(004)-C(007)-H(007)	111.1
C(00D)-C(007)-H(007)	111.1
C(00A)-C(007)-H(007)	111.1
O(001)-C(008)-C(009)	109.85(10)
O(001)-C(008)-H(00A)	109.7
C(009)-C(008)-H(00A)	109.7
O(001)-C(008)-H(00B)	109.7
C(009)-C(008)-H(00B)	109.7
H(00A)-C(008)-H(00B)	108.2
O(002)-C(009)-C(008)	109.67(11)
O(002)-C(009)-H(00C)	109.2(10)
C(008)-C(009)-H(00C)	108.9(10)
O(002)-C(009)-H(00D)	110.2(9)
C(008)-C(009)-H(00D)	109.8(8)
H(00C)-C(009)-H(00D)	108.9(13)
C(00B)-C(00A)-C(007)	109.78(11)
C(00B)-C(00A)-H(00E)	109.7
C(007)-C(00A)-H(00E)	109.7
C(00B)-C(00A)-H(00F)	109.7
C(007)-C(00A)-H(00F)	109.7
H(00E)-C(00A)-H(00F)	108.2
C(00A)-C(00B)-C(006)	109.83(11)
C(00A)-C(00B)-H(00G)	109.7
C(006)-C(00B)-H(00G)	109.7
C(00A)-C(00B)-H(00H)	109.7
C(006)-C(00B)-H(00H)	109.7
H(00G)-C(00B)-H(00H)	108.2
O(002)-C(00C)-H(00I)	109.5
O(002)-C(00C)-H(00J)	109.5
H(00I)-C(00C)-H(00J)	109.5
O(002)-C(00C)-H(00K)	109.5
H(00I)-C(00C)-H(00K)	109.5
H(00J)-C(00C)-H(00K)	109.5
C(007)-C(00D)-C(00E)	110.16(11)
C(007)-C(00D)-H(00L)	109.6
C(00E)-C(00D)-H(00L)	109.6
C(007)-C(00D)-H(00M)	109.6
C(00E)-C(00D)-H(00M)	109.6
H(00L)-C(00D)-H(00M)	108.1
C(006)-C(00E)-C(00D)	109.45(11)
C(006)-C(00E)-H(00N)	109.8
C(00D)-C(00E)-H(00N)	109.8
C(006)-C(00E)-H(00O)	109.8
C(00D)-C(00E)-H(00O)	109.8

H(00N)-C(00E)-H(00O) 108.2

Symmetry transformations used to generate equivalent atoms:
#1 -x+1,-y+1,-z+1

Table S10. Anisotropic displacement parameters U^{ij} ($Å^2 x\ 10^3$) for BODEA. The anisotropic displacement factor exponent takes the form: $-2\pi^2[\ h^2a^2U^{11} + ... + 2\ h\ k\ ab\ U^{12} + \ldots]$

	U^{11}	U^{22}	U^{33}	U^{23}	U^{13}	U^{12}
O(001)	56(1)	51(1)	33(1)	4(1)	22(1)	8(1)
O(002)	66(1)	80(1)	47(1)	-18(1)	27(1)	-19(1)
C(003)	42(1)	43(1)	30(1)	4(1)	16(1)	5(1)
C(004)	36(1)	46(1)	35(1)	4(1)	14(1)	3(1)
C(005)	39(1)	44(1)	31(1)	2(1)	11(1)	2(1)
C(006)	46(1)	64(1)	34(1)	-3(1)	9(1)	-7(1)
C(007)	40(1)	66(1)	47(1)	4(1)	20(1)	-2(1)
C(008)	71(1)	49(1)	48(1)	3(1)	31(1)	9(1)
C(009)	62(1)	53(1)	47(1)	-10(1)	26(1)	-3(1)
C(00A)	38(1)	85(1)	63(1)	5(1)	15(1)	8(1)
C(00B)	42(1)	89(1)	50(1)	12(1)	3(1)	4(1)
C(00C)	68(1)	76(1)	50(1)	-1(1)	29(1)	-1(1)
C(00D)	60(1)	67(1)	66(1)	4(1)	24(1)	-18(1)
C(00E)	69(1)	66(1)	60(1)	-10(1)	17(1)	-20(1)

Table S11. Hydrogen coordinates (x 10^4) and isotropic displacement parameters U(eq) ($Å^2$ x 10^3) for BODEA.

	x	y	z	U(eq)
H(006)	2783	3956	2070	60
H(007)	2027	4385	5786	60
H(00A)	5264	2796	2542	64
H(00B)	6876	3276	3169	64
H(00E)	80	4844	3794	75
H(00F)	1140	6057	4212	75
H(00G)	1635	5899	2476	77
H(00H)	488	4755	2013	77
H(00I)	6697	4340	-557	93
H(00J)	7896	3267	27	93
H(00K)	8306	4773	162	93
H(00L)	955	2553	4432	77
H(00M)	2611	2271	5147	77
H(00N)	2871	2037	3308	79
H(00O)	1234	2400	2594	79
H(00C)	5271(18)	3772(17)	627(15)	72(5)
H(00D)	6241(16)	2471(17)	1009(14)	67(4)

8. References

[1] R. Rathore, J. K. Kochi, *J. Org. Chem.* **1995**, 60, 4399-4411.
[2] U. Andersson, U. W. Gedde, A. Hult, *Molec. Crystals and Liquid Crystals Sci. Techn.* **1994**, 243, 313-321.
[3] J. K. Feng, X. P. Ai, Y. L. Cao, H. X. Yang, *Electrochem. Comm.* **2007**, 9, 25-30.
[4] APEX2 (Bruker Analytical X-ray Instruments, Inc. Madison, Wisconsin, USA., 2005).
[5] Computer code SHELXTL v. version 6.12 (Bruker Analytical X-ray Instruments, Inc. Madison, WI, 2001).